



Cite this: *Dalton Trans.*, 2019, **48**, 17445

Received 24th October 2019,
Accepted 7th November 2019

DOI: 10.1039/c9dt04138a

rsc.li/dalton

Highly efficient Mo₃^{IV}...Sb^{III} cluster frustrated Lewis pair hydrogenation†

Fang Yu^{a,b} and Li Xu^{ID} *^a

Frustrated Lewis pairs (FLPs) featuring Lewis acid–base synergistic action have been recognized as one of the most powerful bifunctional catalytic systems. Each Lewis component, however, is usually composed of a single atom and hence lacks a cooperative effect. In this work, cluster FLPs (CFLPs) comprised of a triangularly Mo–Mo bonded Mo₃^{IV} Lewis acidic cluster component and a Lewis basic Sb^{III} partner in H[Sb₃^{III}Mo₃^{IV}Mo₁₅^{VI}O₅₅(OH)₂py₃] (1) have been developed. The more extensive cooperative actions both within Mo₃^{IV} and between Mo₃^{IV} and Sb^{III} account for the excellent catalytic performance of 1, providing a new way of thinking for the designed synthesis of highly efficient FLP catalysts.

Introduction

Main group FLP hydrogenation initiated by the discovery of the metal-free heterolytic cleavage of dihydrogen is one of the most exciting recent developments in bifunctional catalysis.^{1,2} Later, it has been rapidly broadened to transition metal^{3,4} and rare earth FLPs,⁵ respectively, as they can also serve as Lewis acidic components. These reported FLP systems usually comprise a single Lewis acid–base pair in which each component is composed of a single main group, transition metal or rare earth atom and hence lack a cooperative effect. With this consideration in mind, we propose a new concept: a cluster FLP (CFLP) that comprises Lewis acidic (or basic) cluster components instead of a single atom centre. It features interatomic bonding among neighboring Lewis acidic (or basic) components and hence allows for more extensive synergistic effects not only between the FLP partners but also within the FLP components. Polyoxometalates (POMs) are one of the

most important types of clusters comprising from several to hundreds of oxygen-bridged metal centres.^{6–9} POMs contain numerous Lewis basic bridging/terminal oxygen atoms, but they are not efficient FLP systems because of the absence of active Lewis acid sites. As a consequence, they are widely exploited for catalyzing oxidation reactions but their applications in hydrogenation catalysis (at high temperature¹⁰ or *via* electrochemical reduction¹¹) are extremely rare. Recently, triangularly Mo–Mo bonded Mo₃^{IV} Lewis acidic cluster components have been successfully incorporated into POMs.^{12–15} In contrast to the reported FLP systems bearing strong Lewis basic pnictogenium(III) (Pn^{III}) components,^{1–4} however, they have comparatively weak Lewis basic oxygen partners, which limits their catalytic efficiency in terms of the reaction rate, temperature, catalyst dosage and recyclability. We thus have an idea to incorporate strongly Lewis basic Pn^{III} components into {Mo₃^{IV}}–POM hybrid clusters to enhance both the FLP activity and stability. Herein, we wish to report the first example of CFLPs comprised of Mo₃^{IV}...Pn^{III} Lewis pairs, [Sb₃^{III}Mo₃^{IV}Mo₁₅^{VI}O₅₅(OH)₂py₃]·NH₂(CH₃)₂·4NH(CH₃)₂·2H₂O ({Sb₃^{III}Mo₃^{IV}Mo₁₅^{VI}}-1), which exhibits remarkably enhanced catalytic performance as a consequence of the much more powerful Mo₃^{IV}...Sb^{III} CFLP.

Results and discussion

{Sb₃^{III}Mo₃^{IV}Mo₁₅^{VI}}-1 was obtained by the organic acid-assisted solvothermal oxidative aggregation of [Mo₃O₂(O₂CCH₃)₆(H₂O)₃]²⁺ and heterometallic oxide (Sb₂O₃) (Fig. S1†), presenting a new synthetic strategy to incorporate heteroatoms into CFLP hybrid clusters (Fig. 1). They were initially obtained by the incomplete oxidation of [Mo₃O₄(H₂O)₉]⁴⁺ in a low yield. Later, the more robust bioxo-capped hexaacetate-bridged [Mo₃^{IV}O₂(O₂CCH₃)₆(H₂O)₃]²⁺ was employed to alleviate the Mo₃^{IV} oxidative aggregation by the Mo₃^{IV}(μ₃-O)₂ → Mo₃^{IV}(μ₃-O)(μ₂-O)₃ skeletal conversion,¹⁶ providing a universal preparative route resulting in a much higher and repeatable yield.¹³ As shown in

^aState Key Laboratory of Structural Chemistry, Fujian Institute of Research on the Structure of Matter Chinese Academy of Sciences, Fuzhou, Fujian 350002, P. R. China. E-mail: xli@fjirsm.ac.cn

^bUniversity of Chinese Academy of Sciences, Beijing 100049, China

† Electronic supplementary information (ESI) available: Full experimental and computational details. CCDC 1949159 (1). For ESI and crystallographic data in CIF or other electronic format see DOI: 10.1039/C9DT04138A

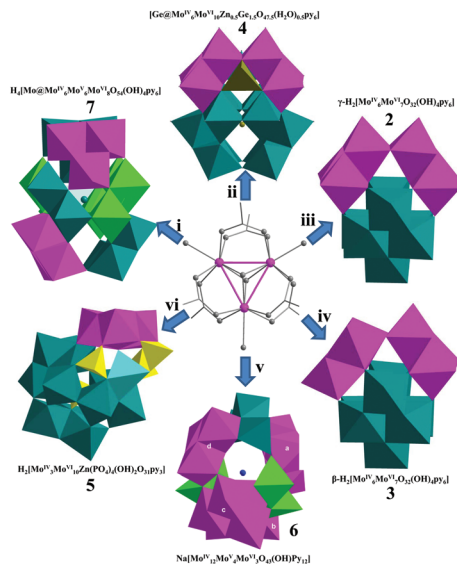


Fig. 1 Solvothermal syntheses of CFLP hybrid clusters 2–7 by the partial oxidative aggregation of the bioxo-capped hexacarboxylate-bridged trimolybdenum(iv) cluster precursor $[\text{Mo}_3^{\text{IV}}\text{O}_2(\text{O}_2\text{CMe})_6(\text{H}_2\text{O})_3]\text{ZnCl}_4$ under different reaction conditions by tuning the components and ratios of mixed solvents, temperature, basic/acidic agents and heterometal oxides (polyhedron color: Mo^{4+} , purple; Mo^{5+} , green; Mo^{6+} , black green; P^{5+} , yellow; Na^+ , blue; Zn^{2+} , aqua; Ge^{4+} , dark yellow). Reaction conditions: (i) py/DMF/ H_2O = 9:1:1, 398 K, 2 days; (ii) py/glycol/ H_2O = 7:1:3, GeO_2 , 421 K, 2 days; (iii) py/DMF/ H_2O = 1:9:1, 348 K, 2 days; (iv) py/EtOH/ H_2O = 8:1:1, 348 K, 2 days; (v) py/MeOH/ H_2O = 7:2:1, Na_2SiO_3 , 421 K, 2 days; (vi) py/ H_2O = 7:3, H_3PO_4 , 409 K, 3 days.

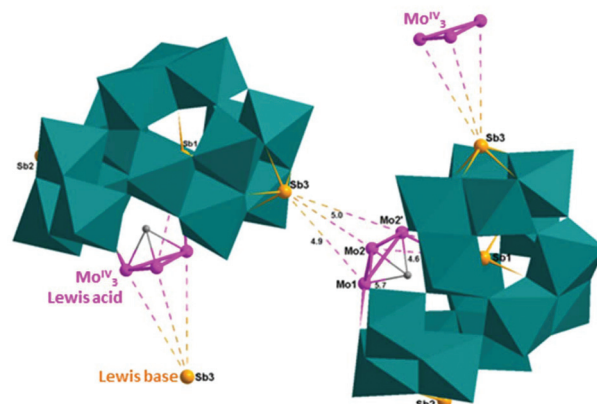


Fig. 2 Chain-like $\text{Mo}_3^{\text{IV}}\dots\text{Sb}^{\text{III}}$ Lewis cluster pairs in the CFLP hybrid cluster $\{\text{Sb}^{\text{III}}\text{Mo}_3^{\text{IV}}\text{Mo}_{15}^{\text{VI}}\}-1$ ($\text{Mo}_3^{\text{IV}}\dots\text{Sb}^{\text{III}}$, 4.5–4.7 Å).

Table 1 Average bond lengths (Å) in CFLP hybrid clusters 1–7 and the discrete 8 and Mo^{IV} -electron transfer ($\Delta\text{Mo}^{\text{IV}}$) based on 8

Clusters	$d(\text{Mo}-\text{Mo})$		$d(\text{Mo}^{\text{IV}}-\mu_2-\text{O}-)$		$\Delta\text{Mo}^{\text{IV}}$
	Mo_3^{IV}	Mo_2^{V}	$-\text{Mo}^{\text{IV}}$	$-\text{M}$	
$\{\text{Sb}_3^{\text{III}}\text{Mo}_3^{\text{IV}}\text{O}_6\text{Mo}_{15}^{\text{VI}}\}-1$	2.527		1.927	2.055	0.245
$\{\gamma-\text{Mo}_6^{\text{IV}}\text{O}_8\text{Mo}_7^{\text{VI}}\}-2$	2.511		1.926	2.087	0.150
$\{\beta-\text{Mo}_6^{\text{IV}}\text{O}_8\text{Mo}_7^{\text{VI}}\}-3$	2.525		1.939	2.090	0.151
$\{\text{Mo}_6^{\text{IV}}\text{O}_2\text{Mo}_{10}^{\text{VI}}\text{Ge}_3\}-4$	2.487		1.930		0.255
$\{\text{Mo}_3^{\text{IV}}\text{O}_7\text{Mo}_{10}^{\text{VI}}\text{P}_4\text{Zn}\}-5$	2.545		1.936	2.088	0.095
$\{\text{Mo}_3^{\text{IV}}\text{O}_5\text{Mo}_1^{\text{VI}}\text{Mo}_9^{\text{VI}}\text{Na}\}-6$	2.512	2.674	1.932	2.011	0.161
$\{\text{Mo}_3^{\text{IV}}\text{O}_6\text{Mo}_6^{\text{VI}}\text{Mo}_9^{\text{VI}}\}-7$	2.506	2.718	1.934	2.062	0.190
$[\text{Mo}_3^{\text{IV}}\text{O}_4(\text{C}_2\text{O}_4)_3\text{Mepy}_3]^{2-}-8$	2.499		1.918		0

Fig. S1,[†] the formation of $\{\text{Sb}_3^{\text{III}}\text{Mo}_3^{\text{IV}}\text{Mo}_{15}^{\text{VI}}\}-1$ can be understood by relating it to non-tetrahedral Dawson variants $[\text{H}_n\text{Pn}^{\text{III}}\text{Mo}_{18}^{\text{VI}}\text{O}_{60}]^{9-n}$ (Pn = pnictide, $n = 2$, Pn = As,¹⁷ $n = 3$, Pn = Bi¹⁸) with an endohedral PnO_3 group. It is monoanionic and charge balance by one protonated dimethyl amine counteranion $\text{NH}_2(\text{CH}_3)_2^+$ most often occurs by the high temperature decomposition of DMF. It is not soluble in water and common organic solvents. As shown in Fig. S2,[†] it exhibits high thermal stability and loses dimethyl amine and water molecules below 300 °C, pyridine dative ligands below 400 °C and molybdenum oxide below 800 °C. The polyhedral representation and atomically labeled structure of $\{\text{Sb}_3^{\text{III}}\text{Mo}_3^{\text{IV}}\text{Mo}_{15}^{\text{VI}}\}-1$ are given in Fig. 2 and S3,[†] respectively. It has crystallographic mirror symmetry (defined by Mo1, Mo10 and three Sb atoms) and features six $[\text{Mo}_3\text{O}_4]$ incomplete cubane-type cluster units one of which marked in purple has three much shorter Mo–Mo bonds (Table 1, av. 2.527(1) Å) than the other five ($\text{Mo}^{\text{VI}}\dots\text{Mo}^{\text{VI}}$, av. 3.333 Å) and is explicitly assigned as the triangular $\text{Mo}^{\text{IV}}-\text{Mo}^{\text{IV}}$ bonded $[\text{Mo}_3^{\text{IV}}\text{O}_4]$ Lewis acidic cluster unit.^{12–15,16,19–21} Each Mo^{IV} is loosely datively bonded to pyridine with weak $\text{Mo}^{\text{IV}}-\text{py}$ bonding (Mo–N 2.24(1), 2.232(7) Å) accounting for the Mo^{IV} Lewis acidic activity.^{12–15} The occurrence of the important electrophilic addition of two Lewis basic Sb^{III} in 6e-reduced $\{\text{Sb}_3^{\text{III}}\text{Mo}_3^{\text{IV}}\text{Mo}_{15}^{\text{VI}}\}-1$ as compared to the parent $\{\text{Pn}^{\text{III}}\text{Mo}_{18}^{\text{VI}}\}$ ^{17,18} is driven by both the charge balance requirement and the more

negative charge of the bridging oxygen atoms (O_b) induced by the 6e-reduction. The endohedral SbO_3 has considerably shorter Sb–O distances (1.958(8) and 1.988(5) Å) than SbO_4 (1.993(8)–2.140(5) Å) and $[\text{P}_2\text{Mo}_{12}\text{Sb}_2^{\text{III}}\text{O}_{40}]^{2-}$ (2.076(5)–2.094(5) Å).²² There are two protons within the cage that are attached to the two capping oxygen atoms (O_{25} and its equivalent) revealed by a low BVS value (1.169, Table S1[†]).

The crystal structure of **1** is given in Fig. S4.[†] It is crucial that the crystal packing of $\{\text{Sb}_3^{\text{III}}\text{Mo}_3^{\text{IV}}\text{Mo}_{15}^{\text{VI}}\}-1$ occurs in such a capping manner that the Lewis basic Sb_3 and Lewis acidic Mo_3^{IV} form chain-like $\text{Mo}_3^{\text{IV}}\dots\text{Sb}^{\text{III}}$ CFLPs as shown in Fig. 2, wherein the Mo_3^{IV} triangles are capped by Sb_3 at distances (4.6, 5.0 Å) similar to the sum of their Allinger's van der Waals radii (4.91 Å). Such capping distances are perfect for cooperatively promoting the heterolytic cleavage of hydrazine substrates between them to produce active hydride and proton intermediates for transfer hydrogenation as detailed below.

DFT theoretical calculations of **1** have been conducted using B3LYP-6-31G*(C,H,O,N)/LanL2DZ (Mo, Sb) on the optimized geometry of the anionic $[\text{Sb}_3^{\text{III}}\text{Mo}_3^{\text{IV}}\text{Mo}_{15}^{\text{VI}}\text{O}_{55}(\text{OH})_2\text{py}_3]^-$ nanocage. The Mo^{IV} atoms have an averaged Mulliken charge of 1.462 (Mo1, 1.521; Mo2, 1.433), which results in an appropriate electron transfer of 0.245 from each Mo^{IV} Lewis acid in contrast to **8** (Mo^{IV} , 1.217). Such Mo^{IV} -electron transfer is

Table 2 Relationship between the selectivity and the yield of CFLPs 1–7 and $\text{Mo}_{3n}^{\text{IV}}-\mu_2-\text{O}_x$ Lewis pairs, heterometal M and HOMO, related catalysts 8 and 9 and catalyst-free conditions are also included for comparison

CFLP catalysts 1–7 and related catalysts 8 and 9	$\text{Mo}_{3n}^{\text{IV}}-\text{O}_x$		$\{\text{Mo}_3^{\text{IV}}\}_n$ linkage	M	HOMO Mo (%)	Catalysis ^a (%)	
	<i>n</i>	<i>x</i>				Selectivity	Yield
$\{\text{Sb}_3^{\text{III}}\text{Mo}_3^{\text{IV}}\text{O}_6\text{Mo}_{15}^{\text{VI}}\}$ -1	1	6	—	Sb^{III}	65.4 Mo^{IV}	100	100
$\{\gamma\text{-Mo}_6^{\text{IV}}\text{O}_8\text{Mo}_7^{\text{VI}}\}$ -2	2	8	γ	—	67.4 Mo^{IV}	99.8	99.8
$\{\beta\text{-Mo}_6^{\text{IV}}\text{O}_8\text{Mo}_7^{\text{VI}}\}$ -3	2	8	β	—	65.6 Mo^{IV}	99.8	78.0
$\{\text{Mo}_2^{\text{IV}}\text{O}_2\text{Mo}_{10}^{\text{VI}}\text{Ge}_3\}$ -4	2	2	γ	Ge^{IV}	59.3 Mo^{IV}	99.8	46.9
$\{\text{Mo}_3^{\text{IV}}\text{O}_7\text{Mo}_{10}^{\text{VI}}\text{P}_4\text{Zn}\}$ -5	1	7	—	$\text{Zn}^{\text{II}}, \text{P}^{\text{V}}$	62.1 Mo^{IV}	97.4	47.9
$\{\text{Mo}_3^{\text{IV}}\text{O}_5\text{Mo}_8^{\text{VI}}\text{Na}\}$ -6	4	5	α, β	Na^+	58.6 Mo^{IV}	99.8	40.8
$\{\text{Mo}_6^{\text{IV}}\text{O}_6\text{Mo}_6^{\text{VI}}\text{Mo}_9^{\text{VI}}\}$ -7	2	6	—	—	56.2 Mo^{V}	97.7	16.8
$[\text{Mo}_3^{\text{IV}}\text{O}_4(\text{C}_2\text{O}_4)_3\text{Mepy}_3]^{2-}$ -8					68.3 Mo^{IV}	14.2	3.9
Sb_2O_3 -9							<5
No							<0.5

^a GC yield, nitrobenzene (10 μL , 0.097 mmol), $\text{N}_2\text{H}_4\cdot\text{H}_2\text{O}$ (85%, 20 μL , 0.3 mmol), EtOH (2 mL), 1, 1 mol%, 60 $^\circ\text{C}$, 0.5 h; 2–9, 3 mol%, 80 $^\circ\text{C}$, 2 h.

helpful to enhance both the Lewis acidity of Mo^{IV} and the Lewis basicity of the surrounding oxygen and heterometal atoms. Also notable are HOMO compositions in which the Mo^{IV} contributions are essential to catalytic activity.¹⁵ As shown in Table 2 and Fig. S5,† the HOMO of 1 is mainly composed of Mo^{IV} (65.4%) as in the cases of 2–6, differing from the HOMO of 7 that is dominated by Mo^{V} (56.2%) and is believed to responsible for the unusually low catalytic activity.

A comparison of the catalytic performance of the CFLP hybrid clusters 1–7 and related compounds 8 and 9 in the hydrazine-mediated transfer hydrogenation of nitrobenzene to aniline, one of the most important industrial hydrogenation reactions,²³ is given in Table 2. Their catalytic efficiency is largely dependent on the number and arrangement of Lewis acidic $\{\text{Mo}_3^{\text{IV}}\}_n$ active units because of the weak Lewis basic oxygen partners when additional Lewis basic partners are absent for 2–7 (Fig. S6†).¹⁵ The head-to-head γ -linkage between two neighboring Mo_3^{IV} triangles (Fig. S7†) allows for the most effective three pairs of $\text{Mo}^{\text{IV}}-\text{Mo}^{\text{IV}}$ synergistic actions, accounting for the best catalytic performance of $\{\gamma\text{-Mo}_6^{\text{IV}}\text{Mo}_7^{\text{VI}}\}$ -2 (yield > 99.8%, Table 2).^{14,15} $\{\text{Mo}_3^{\text{IV}}\text{Mo}_{10}^{\text{VI}}\text{P}_4\text{Zn}^{\text{II}}\}$ -5 containing a single Mo_3^{IV} Lewis acidic unit results in only moderate yield (47.9%), although it also exhibits excellent selectivity (>97%). Like $\{\text{Mo}_3^{\text{IV}}\text{Mo}_{10}^{\text{VI}}\text{P}_4\text{Zn}^{\text{II}}\}$ -5, $\{\text{Sb}_3^{\text{III}}\text{Mo}_3^{\text{IV}}\text{Mo}_{15}^{\text{VI}}\}$ -1 has only one Mo_3^{IV} active Lewis acidic unit. However, the additional stronger Sb^{III} Lewis base offers us a unique opportunity to examine the contribution of the Lewis basic partners to the CFLP system. As indicated in Table 2, $\{\text{Sb}_3^{\text{III}}\text{Mo}_3^{\text{IV}}\text{Mo}_{15}^{\text{VI}}\}$ -1 exhibits perfect selectivity (100%) and conversion (100%) although it has only a single Mo_3^{IV} Lewis acidic unit. Moreover, it also exhibits excellent catalytic efficiency (Fig. 3, yield, 99.8%) at room temperature, which is much higher than that of $\{\gamma\text{-Mo}_6^{\text{IV}}\text{Mo}_7^{\text{VI}}\}$ -2 (yield, 5.8%). The Sb^{III} -enhanced catalytic activity is also revealed by a comparison of catalyst (mol%)-yield plots as shown in Fig. 4. 0.5–3 mol% 1 retains the perfect catalytic performance (yields > 99%) even at 60 $^\circ\text{C}$, whereas 0.5 mol% 2 results in only 36% yield at 80 $^\circ\text{C}$. 0.1 and 0.33 mol% 1 result in 90.9% and 92.9% yields accompanied by unreacted PhNO_2 and the byproduct azoxybenzene, respectively (Fig. S8†), which are much greater

yield at 80 $^\circ\text{C}$. 0.1 and 0.33 mol% 1 result in 90.9% and 92.9% yields accompanied by unreacted PhNO_2 and the byproduct azoxybenzene, respectively (Fig. S8†), which are much greater

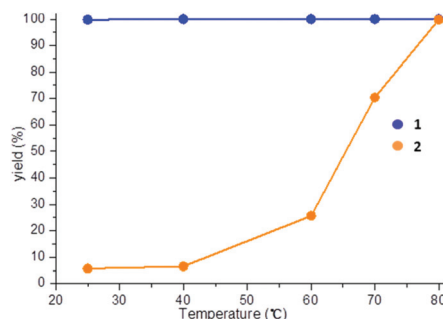


Fig. 3 Catalytic yields of 1 and 2 at different temperatures. Reaction conditions: catalysts, 3 mol%, PhNO_2 , 10 μL , 0.097 mmol, $\text{N}_2\text{H}_4\cdot\text{H}_2\text{O}$, 20 μL , 0.3 mmol, EtOH, 2 mL, 2 h.

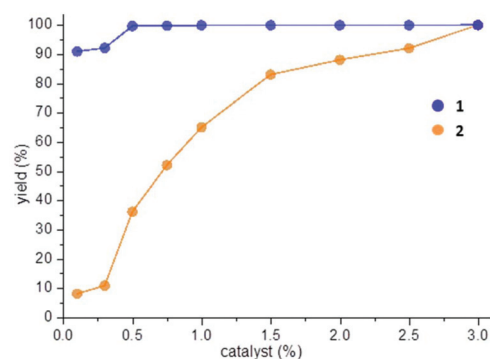


Fig. 4 Catalyst (0.1–3 mol%)-dependent yields for the hydrogenation of nitrobenzene to aniline, reaction conditions: PhNO_2 , 10 μL , 0.097 mmol, $\text{N}_2\text{H}_4\cdot\text{H}_2\text{O}$, 20 μL , 0.3 mmol, EtOH, 2 mL, 2 h, 1, 60 $^\circ\text{C}$, 2, 80 $^\circ\text{C}$.

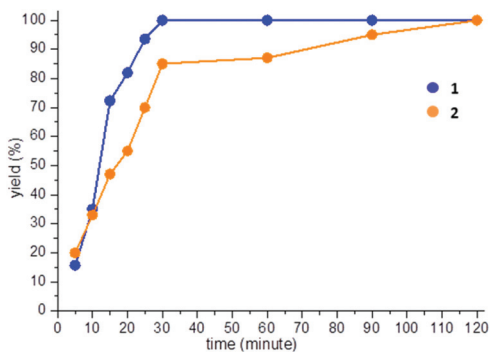


Fig. 5 Time-dependent catalysis yields for the hydrogenation of nitrobenzene to aniline. Reaction conditions: catalysts, 3 mol%, PhNO₂, 10 μL, 0.097 mmol, N₂H₄·H₂O, 20 μL, 0.3 mmol, EtOH, 2 mL, 80 °C.

than the 8.0% yield obtained using 0.1 mol% 2. A comparison of time–yield plots (Fig. 5 and Fig. S9†) further indicates the highly improved catalytic performance of {Sb^{III}Mo₃Mo^{IV}Mo₁₅^{VI}}-1 that achieves complete conversion within 30 minutes in contrast to 120 minutes required for {γ-Mo^{IV}Mo₇^{VI}}-2. Notable is the initial (<5 min) formation of the PhNHOH intermediate for the former (Fig. S9†), which reveals the direct multiple route (Scheme S1†) as in the case of the latter. The absence of the PhNHOH intermediate for the latter may be related to the two Mo^{IV} Lewis acidic active units that stabilize up to six hydrides allowing for the complete conversion of PhNO₂ to PhNH₂ and 2H₂O in each catalysis cycle.¹⁴ The remarkably enhanced performance of {Sb^{III}Mo₃Mo^{IV}Mo₁₅^{VI}}-1 is believed to be related to the stronger Lewis basicity and higher stability of the Sb^{III} partners promoting and presumably dominating the bifunctional synergistic actions of the Mo^{IV}...Sb^{III} CFLPs catalyzing Sb: → H⁺ → N → H⁻ → Mo^{IV} heterolytic cleavage of hydrazine. Such Mo^{IV}...Sb^{III} CFLP synergistic actions for generating and stabilizing the proton/hydride intermediates obtained by hydrazine heterolysis play an essential role in the excellent catalytic performance since both Sb₂O₃ and the discrete Mo₃O₄-type cluster **8** have very low activity (yield < 5%, Table 2). Table 3 and Fig. S10† describe the influence of the nitroarene substituents on the catalysis yields of {Sb^{III}Mo₃Mo^{IV}Mo₁₅^{VI}}-1. The Lewis basic substituents *trans* to NO₂ remarkably reduce the catalytic activity as revealed by the lowest yield (39.2%) with the strongest basicity (*trans*-NH₂). This might indicate the essential role of the Lewis acidic Mo₃^{IV} partners that can be deactivated by the non-frustrated -HN₂ Lewis base. The yield of the *cis*-OH derivative (99.8%) is much higher than that of the *trans*-OH derivative (61.2%) presumably as a consequence of the inner OH...O₂N hydrogen bond and the resulting steric hindrance of the former which reduce the Lewis basicity and the Mo^{IV}-bonding ability of the *cis*-OH group. The recyclability of the insoluble {Sb^{III}Mo₃Mo^{IV}Mo₁₅^{VI}}-1 heterogeneous catalyst has been examined as shown in Fig. 6, S11 and S12.† It exhibits both perfect selectivity (100%) and excellent conversion (>95%) for cycles 1–10, and hence shows much better recyclable performance than {γ-Mo^{IV}Mo₇^{VI}}-2

Table 3 Hydrazine-mediated hydrogenation of nitroarenes to arylamines catalysed by {Sb^{III}Mo₃Mo^{IV}Mo₁₅^{VI}}-1^a

Entry	Reaction	Yield (%)
1		99.8
2		99.8
3		99.8
4		99.8
5		99.8
6		99.8
7		81.2
8		61.2
9		39.2

^a Determined by GC-2014, reaction conditions: nitrobenzene (10 μL, 0.097 mmol), N₂H₄·H₂O (20 μL, 0.3 mmol), 3 mol% catalysts, EtOH (2 mL), 2 h.

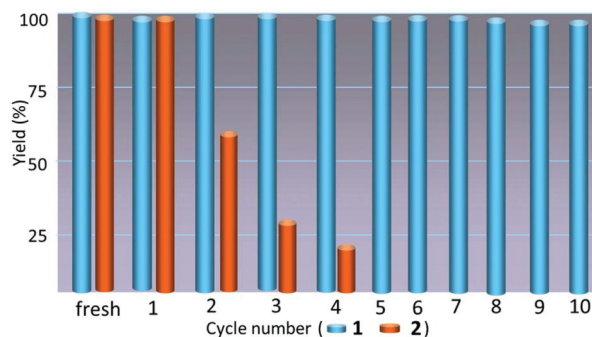


Fig. 6 Recyclability of **1** and **2** in the heterogeneous catalysis hydrogenation of nitrobenzene to aniline. Catalysis conditions: 3 mol%, PhNO₂, 10 μL, 0.097 mmol, N₂H₄·H₂O, 20 μL, 0.3 mmol, EtOH, 2 mL, 80 °C, for **1**: fresh and cycle 1, 0.5 h, cycle 2, 1 h, cycles 3–10, 2 h. For **2**: fresh and cycles 1–4, 2h.

under similar catalysis conditions. The markedly improved recyclability of {Sb^{III}Mo₃Mo^{IV}Mo₁₅^{VI}}-1 can be assigned to the more stable Sb^{III} Lewis basic sites that may largely contribute to the Mo^{IV}...Sb^{III} CFLP activity.

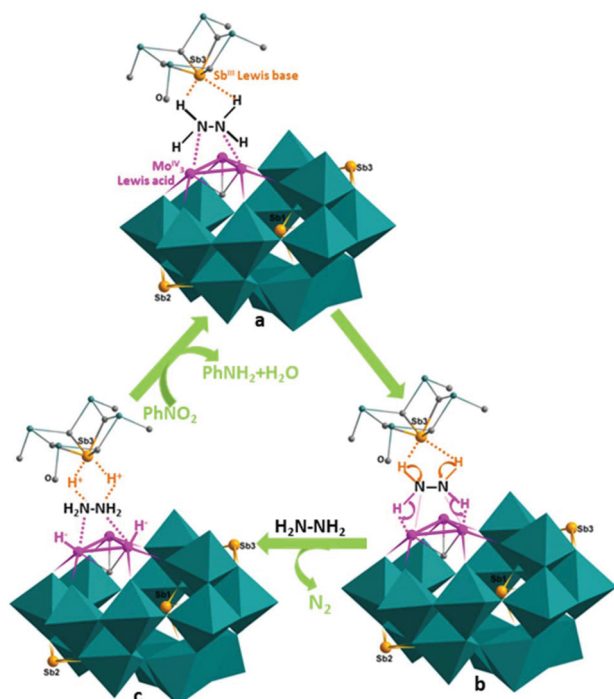


Fig. 7 The proposed catalytic cycle for $\{Sb_3^{III}Mo_3^{IV}Mo_{15}^{VI}\}O_{55}(OH)_2py_3-1$ promoting the hydrazine transfer hydrogenation of nitrobenzene to aniline. (a) Hydrazine coordination to Lewis basic Sb^{III} and Lewis acidic Mo_3^{IV} through pyridine substitution. (a) \rightarrow (b) $Mo_3^{IV}-Sb^{III}$ FLP promoted $H^+ \rightarrow N \rightarrow H^-$ hydrazine heterolysis. (b) \rightarrow (c) Formation of $Mo^{IV}-H^-$ hydrides and $Sb^{III}-H^+$ intermediates accompanied by the release of N_2 . (c) \rightarrow (a) Hydride and proton transfer hydrogenation of $PhNO_2$ to $PhNH_2$ and H_2O followed by the next catalytic cycle.

With the above considerations in mind and the appropriate intermolecular $Sb_3 \cdots Mo_3^{IV}$ distances (Fig. 2), we propose the following catalytic cycle of $\{Sb_3^{III}Mo_3^{IV}Mo_{15}^{VI}\}O_{55}(OH)_2py_3-1$ promoting the hydrazine-mediated transfer hydrogenation of nitrobenzene to aniline as depicted in Fig. 7: initially, the pyridine ligands loosely attached to Mo_3^{IV} are replaced by hydrazine (Fig. 7a). The subsequent dual $H^+ \rightarrow N \rightarrow H^-$ heterolysis of the bridging N_2H_4 through the transition state (Fig. 7b) promoted by the synergistic actions of the $Sb^{III} \cdots Mo_3^{IV}$ CFLPs leads to the generation of $Mo^{IV}H^-$ hydride and $Sb^{III}H^+$ ($Mo^{VI}OH^+$ and/or $H^+_2N_2H_4$) intermediates (Fig. 7c) accelerated by the release of N_2 . The last multi-step (c \rightarrow a) closes the cycle *via* the hydride and proton transfer hydrogenation of nitrobenzene to aniline and starts the next catalytic cycle. The counteraction $[H_2N(CH_3)_2]^+$ may also be involved in the proton transfer process.

Conclusion

A new concept of a CFLP featuring more extensive cooperative actions both within the Lewis cluster components and between the Lewis cluster partners has been proposed, unveiling a new way of thinking for the designed synthesis of high-performance FLP catalysts. This has been supported by the

excellent catalytic performance of the CFLP hybrid cluster $H[Sb_3^{III}Mo_3^{IV}Mo_{15}^{VI}O_{55}(OH)_2py_3]$ as a consequence of the extensive synergistic effects both within the Lewis acidic Mo_3^{IV} cluster component and between Mo_3^{IV} and Sb^{III} Lewis basic partners.

Conflicts of interest

There are no conflicts to declare.

Acknowledgements

This work is supported by the National Natural Science Foundation of China (21873102) and the Strategic Priority Research Program of Chinese Academy of Sciences, Grant No. XDB 20000000.

References

- 1 D. W. Stephan, *Science*, 2016, **354**, aaf7229.
- 2 J. Lam, K. M. Szkop, E. Mosaferi and D. W. Stephan, *Chem. Soc. Rev.*, 2018, **48**, 3592–3612.
- 3 O. Tutusaus, C. B. Ni and N. K. Szymczak, *J. Am. Chem. Soc.*, 2013, **135**, 3403–3406.
- 4 S. R. Flynn and D. F. Wass, *ACS Catal.*, 2013, **3**, 2574–2581.
- 5 Y. Y. Ma, S. Zhang, C.-R. Chang, Z.-Q. Huang, J. C. Ho and Y. Q. Qu, *Chem. Soc. Rev.*, 2018, **47**, 5541–5553.
- 6 H. N. Miras, J. Yan, D. L. Long and L. Cronin, *Chem. Soc. Rev.*, 2012, **41**, 7403–7430.
- 7 L. Chen, W. L. Chen, X. L. Wang, Y. G. Li, Z. M. Su and E. B. Wang, *Chem. Soc. Rev.*, 2019, **48**, 260–284.
- 8 S. S. Wang and G. Y. Yang, *Chem. Rev.*, 2015, **115**, 4893–4962.
- 9 Y. F. Song and R. Tsunashima, *Chem. Soc. Rev.*, 2012, **41**, 7384–7402.
- 10 (a) H. Benaissa, P. N. Davey, Y. Z. Khimiyak and I. V. Kozhevnikov, *J. Catal.*, 2008, **253**, 244–252; (b) H. Benaissa, P. N. Davey, E. F. Kozhevnikova and I. V. Kozhevnikov, *Appl. Catal., A*, 2008, **351**, 88–92; (c) F. Lin and Y. H. Chin, *J. Catal.*, 2016, **341**, 136–148.
- 11 L. MacDonald, B. Rausch, M. D. Symes and L. Cronin, *Chem. Commun.*, 2018, **54**, 1093–1096.
- 12 W. P. Chen, R. L. Sang, Y. Wang and L. Xu, *Chem. Commun.*, 2013, **49**, 5883–5885.
- 13 X. Xu, B. L. Luo, L. L. Wang and L. Xu, *Dalton Trans.*, 2018, **47**, 3218–3222.
- 14 B. L. Luo, R. L. Sang, L. F. Lin and L. Xu, *Catal. Sci. Technol.*, 2019, **9**, 65–69.
- 15 B. L. Luo and L. Xu, *Dalton Trans.*, 2019, **48**, 6892–6898.
- 16 (a) L. Xu, H. Liu, D. C. Yan, J. S. Huang and Q. E. Zhang, *J. Chem. Soc., Chem. Commun.*, 1993, 1507–1510; (b) L. Xu, Z. H. Li, H. Liu, J. S. Huang and Q. E. Zhang, *Chem. – Eur. J.*, 1997, **3**, 226–231; (c) L. Xu, H. Liu, D. C. Yan, J. S. Huang and Q. E. Zhang, *J. Chem. Soc., Dalton Trans.*, 1994, 2099–

- 2107; (d) L. Xu, Z. F. Li and J. S. Huang, *Inorg. Chem.*, 1996, **35**, 5097–5100.
- 17 Y. Jeannin and J. M. Frere, *Inorg. Chem.*, 1979, **18**, 3010–3014.
- 18 Y. Ozawa and Y. Sasaki, *Chem. Lett.*, 1987, 923–926.
- 19 D. T. Richens, *The Chemistry of Aqua Ions*, John Wiley & Sons, Chichester, 1997.
- 20 (a) F. A. Cotton, D. O. Marler and W. Schwotzer, *Inorg. Chem.*, 1984, **23**, 3671–3673; (b) B. Modec and P. Bukovec, *Inorg. Chim. Acta*, 2015, **424**, 226–234.
- 21 J. Li, C. W. Liu and J. X. Lu, *J. Chem. Soc., Faraday Trans.*, 1994, **90**, 39–45.
- 22 (a) R. Bakri, A. Booth, G. Harle, P. S. Middleton, C. Wills, W. Clegg, R. W. Harrington and R. J. Errington, *Chem. Commun.*, 2012, **48**, 2779–2781; (b) S.-Y. Shi, Y.-H. Sun, Y. Chen, J.-N. Xu, X.-B. Cui, Y. Wang, G.-W. Wang, G.-D. Yang and J.-Q. Xu, *Dalton Trans.*, 2010, **39**, 1389–1394.
- 23 (a) H. J. Arpe, *Industrial Organic Chemistry*, Wiley-VCH, Weinheim, 5th edn, 2010; (b) *Modern Reduction Methods*, ed. P. G. Andersson and I. J. Munslow, Wiley-VCH Verlag GmbH & Co. KGaA, Weinheim, 2008; (c) *Catalytic Hydrogenation*, ed. L. Cervený, Elsevier, Amsterdam, 1986.